The Starburst–AGN Connection
ASP Conference Series, Vol. 408, © 2009
Weimin Wang, Zhaoqing Yang, Zhijian Luo, and Zhu Chen, eds.

Luminous Infrared Galaxies and the "Starburst-AGN Connection"

D. B. Sanders, J. S. Kartaltepe, L. J. Kewley, U. Vivian, T. Yuan

Institute for Astronomy, University of Hawaii, Honolulu, HI 96822, USA E-mail: sanders@ifa.hawaii.edu

A. S. Evans

Department of Astronomy, University of Virginia, Charlottesville, VA 22901, USA E-mail: aevans@virginia.edu

L. Armus, J. M. Mazzarella

IPAC/SSC, California Institute of Technology, Pasadena, CA 91125, USA E-mail: mazz@ipac.caltech.edu, lee@ipac.caltech.edu

Abstract. Luminous Infrared Galaxies (LIRGs) represent perhaps the most powerful examples of a connection between the fueling of starbursts and active galactic nuclei (AGNs). Major mergers of gas-rich spirals, which are now understood to trigger the majority of LIRGs, drive the bulk of the disk gas into the central kpc of the merger pair, where it provides fuel for both powerful nuclear starbursts and accretion onto a central massive black hole. The combined feedback from starburst and accretion luminosity eventually expels the gas, shutting down nuclear activity and leaving a gas-poor elliptical. Although there is now general agreement on the origin and evolutionary scenario for LIRGs, the detailed time evolution of starburst activity and black hole growth is still not well understood. We review the basic properties of LIRGs as determined from extensive multi-wavelength studies of a complete sample of local objects, and introduce new results from initial observations of fainter more distant LIRGs detected in the *Spitzer* survey of the *HST*-COSMOS 2-deg^2 Field.

1. Introduction

Luminous Infrared Galaxies (LIRGs: $\log(L_{\rm IR}/L_\odot > 11.0)$[1] are now widely understood to represent an extremely important class of extragalactic objects that are directly linked to major episodes in galaxy building and transformation. In particular, ultraluminous infrared galaxies (ULIRGs: $\log(L_{\rm IR}/L_\odot > 12.0)$) appear to represent a transition stage near the end phase of the major merger of gas-rich $\sim L^*$ spirals in the process of forming a massive elliptical. Multi-wavelength studies of large samples of (U)LIRGs have shown that both powerful nuclear starbursts and accretion onto a massive black hole (MBH) can play major roles in producing the enormous observed infrared luminosity.

It should become obvious during this Workshop, as LIRGs are featured in many of the presentations, that multi-wavelength studies of LIRGs are forcing us to accept the hypothesis that a close connection may exist between the fuel-

[1] $L_{\rm IR} \equiv L(8-1000\mu{\rm m})$; see Sanders & Mirabel 1996 (SM96) for a more complete description.

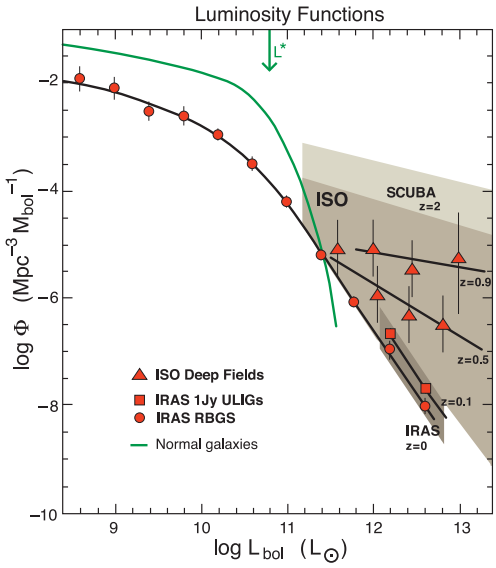

Figure 1. The luminosity functions (LFs) for IR-selected galaxies. The thick solid curve and filled circles represent the local LF as determined from all galaxies in the IRAS RBGS (Sanders et al. 2003). The thin curve represents the LF for optically selected normal galaxies in the local Universe (Schechter 1976). In the luminosity range log $(L_{\rm IR}/L_{\odot}) = 11.0 - 11.4$, IR-galaxies are rapidly becoming a significant population of all extragalactic objects (increasing from ∼10% to ∼50%), and at log $(L_{\rm IR}/L_{\odot}) > 11.4$, they dominate over the rapidly declining high-luminosity tail of the Schechter function. But more importantly, it is this high-luminosity tail of the IR-galaxy LF that exhibits strong evolution with redshift, increasing by 200-1000× from $z = 0$ to $z = 2.5$, as illustrated by IRAS 1-Jy sample (Kim & Sanders 1998) and the shaded ISO (e.g. Sanders 2003, Jacobs et al. 2009) and SCUBA regions.

ing of circumnuclear starbursts and AGN. It seems appropriate in this opening presentation to first briefly review the general properties of infrared galaxies – luminosity functions (LFs), spectral energy distributions (SEDs) – in order to properly place (U)LIRGs in the cosmological framework of extragalactic objects. We then summarize the properties of individual objects, including new results from our two large multi-wavelength surveys of (U)LIRGs: (1) the Great Observatories All-sky LIRG Survey (GOALS: Armus et al. 2009)[2], and (2) the *Spitzer*-COSMOS Survey (S-COSMOS: Sanders et al. 2007)[3] - which focus on the properties of low-z and high-z sources, respectively.

2. Luminosity Functions and Spectral Energy Distributions

Much of what we currently know about luminous infrared galaxies comes from studies of objects detected in the *Infrared Astronomical Satellite* (IRAS) All-Sky Survey (Neugebauer et al. 1984). Fig. 1 shows the local infrared LF determined

[2]http://goals.ipac.caltech.edu/

[3]http://cosmos.astro.caltech.edu/

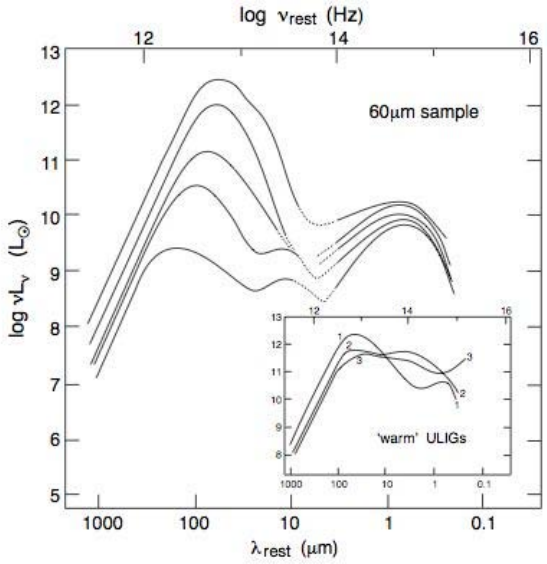

Figure 2. The variation of the mean SEDs (submm-to-UV) with increasing $L_{\rm IR}$ for a 60 μm-selected sample of infrared galaxies (c.f. SM96). The insert shows examples of the subset ($\sim$15%) of ULIRGs which exhibit "warm" infrared color ($f_{25}/f_{60} > 0.3$). Data for the 3 objects (1−the powerful Wolf-Rayet galaxy IRAS 01002-2238, 2−the "IR QSO" IRAS 07598+6508, 3−the optically selected QSO I Zw 1) are from Sanders et al. (1988a,b)

from 60μm-selected RBGS and 1-Jy samples, illustrating the prominent high-luminosity tail of objects that dominate over the rapidly declining population of optically selected galaxies at similar bolometric luminosities. Subsequent, more sensitive surveys with the *Infrared Space Observatory* (ISO), and the *Spitzer Space Telescope*, as well as new submillimeter surveys with the SCUBA submm camera on the James Clerk Maxwell Telescope (JCMT) on Mauna Kea, have allowed us to trace the evolution of the infrared LF versus redshift, which appears to show strong evolution over the range $z \sim 0 - 2$. Studying the low-z IRAS galaxies at log $(L_{\rm IR}/L_\odot) > 11.0$ may offer us the best chance of understanding the properties of their much more numerous, higher-z analogs, which at $z \sim 2$ may actually dominate the total luminosity output of all galaxies.

Fig. 2 shows the mean SEDs of infrared-selected galaxies, illustrating both the similarity in the mean SEDs for rest frame 60μm-selected galaxies (the prominent FIR-submm dust emission and stellar bump at optical-NIR wavelenghts), as well as the differences (e.g. warmer dust with increasing $L_{\rm IR}$). In addition, infrared surveys at shorter wavelengths (e.g. 25μm) clearly favor objects with much warmer dust emission characteristic of heating from an AGN.

2.1. The *Spitzer*-COSMOS Survey

The first comprehensive and systematic identifications of large samples of LIRGs at high redshift are now possible using several new deep surveys that have recently been carried out with the *Spitzer Space Telescope*. Multi-wavelength

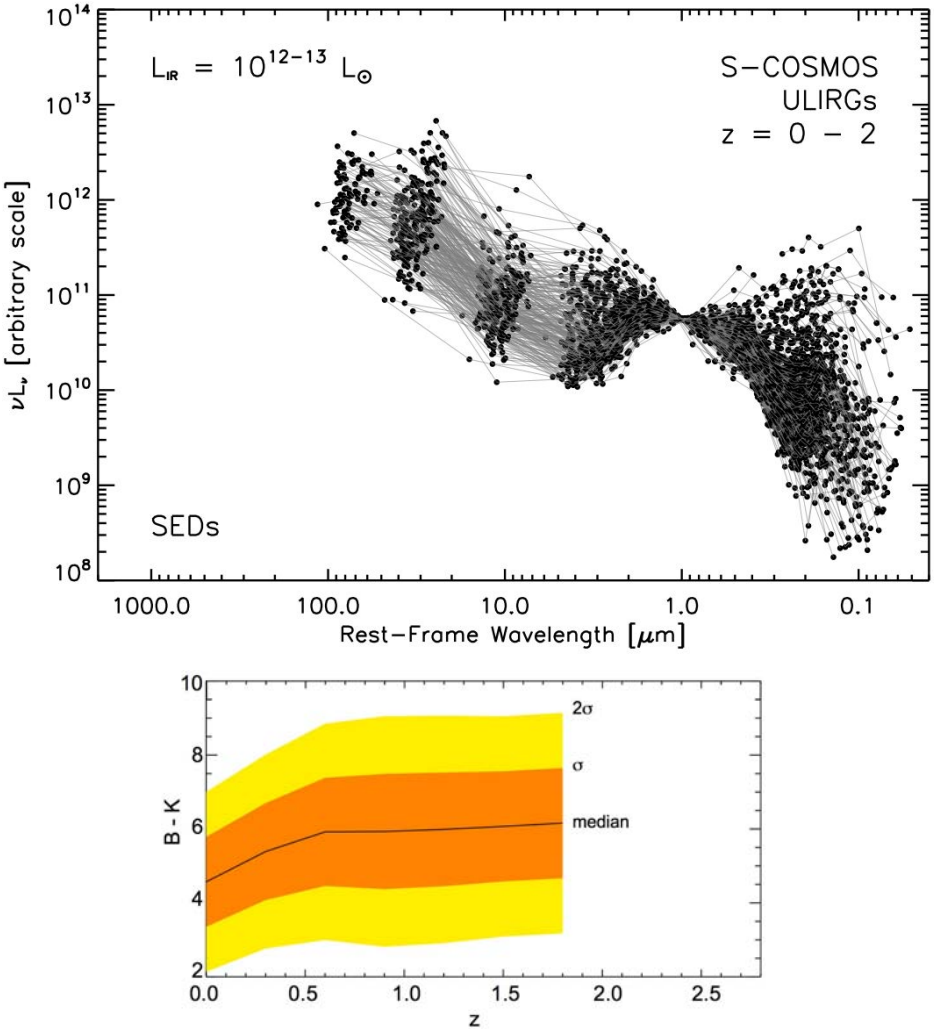

Figure 3. *(Top panel):* FUV-to-FIR SEDs for a complete sample of 70 μm-selected ULIRGs (Kartaltepe 2009) from the *Spitzer*-COSMOS Survey (Sanders et al. 2007, Frayer et al. 2009) of the *HST*-COSMOS 2-deg^2 Field (Scoville et al. 2007). The stacked SEDs have been normalized at 1 μm and are displayed in the object rest-frame. The objects range in redshift from $z \sim 0.3-2.0$, thus the 70 μm-selection corresponds to a $\sim 23-54$ μm-selection in the object rest-frame. The stacked spectra illustrate the range of ULIRG colors at FUV-opt ($\sim$500$\times$), NIR-MIR ($\sim$30$\times$), and MIR-FIR ($\sim$10$\times$) wavelengths. *(Bottom panel):* The range of rest-frame opt-NIR color, $(B-K)$, exhibited by the ULIRGs as a function of redshift (U et al. 2009).

imaging and spectroscopy campaigns are currently underway by several research teams in an attempt to characterize the properties of high-z LIRGs in order to better understand the cosmic evolution of dusty starbursts and dust enshrouded AGN, and their contribution to the total luminosity budget of all galaxies over cosmic time.

Fig. 3 shows initial results from our own *Spitzer*-MIPS survey of the *HST*-ACS COSMOS 2-deg^2 Field. A large sample of ∼1400 70μm-selected galaxies (Kartaltepe 2009) have been identified, their multi-wavelength spectral energy distributions (SEDs) compiled, morphologies determined, and redshifts measured and/or computed using the extensive COSMOS data set (see Kartaltepe et al., this volume). Although the median SED for ULIRGs in the COSMOS Field is similar to that shown for local ULIRGs in Fig. 2, the full range of SED shapes and rest-frame colors can be quite dramatic, particularly at FUV-optical wavelengths, but also in the mid-IR. The data also show that attempts to identify (U)LIRGs in NIR-optical surveys based on using single templates of well-known local objects (e.g. the "cool" ULIRG Arp 220, or "warm" ULIRG Mrk 231) are inadequate, and need to be replaced by a broader range of colors versus redshift such as illustrated in the bottom panel of Fig. 3.

3. The Origin and Evolution of (U)LIRGs

Multi-wavelength studies of complete samples of infrared-selected galaxies in the local universe have made it very clear that strong interactions and mergers of gas-rich spirals are responsible for producing the most luminous infrared objects, while minor mergers make a substantial contribution to the population of lower luminosity LIRGs. Similar studies of more distant objects selected from deep surveys with *Spitzer* are now underway to test whether similar processes are implicated at higher redshift, while studies of even more distant objects ($z \sim 3-5$) detected in mm-submm surveys are attempting to determine how these objects are related to lower redshift (U)LIRGs. Here we choose to focus on a few of the new results that are being obtained for nearby (U)LIRGs, which will hopefully allow us to construct a more complete picture of these objects that can then be compared with more detailed studies of the more distant (U)LIRGs once higher resolution data for these objects (e.g. using EVLA, ALMA, ...) become available.

3.1. High Resolution *HST* Imaging

Fig. 4 shows a set of the new I-band *HST*-ACS images from the *HST*-GOALS B, I-band imaging survey (Evans et al. 2009), arranged in order of increasing infrared luminosity to better illustrate the general progression from early merger to late stage merger with increasing $L_{\rm IR}$. The prominent tidal tails and relatively large galaxy pairs seen in most images are characteristic of major (<3:1) $\sim L^* - L^*$ mergers. The ACS resolution is sufficient to resolve numerous star clusters and to better delineate connecting bridges, loops, fans, and rings, which allows us to more accurately reconstruct merger kinematics and geometry. By coupling these high resolution images with additional high resolution multi-wavelength spectroscopic and imaging data we hope to be able to construct a much more accurate picture of the time evolution of starburst activity through-

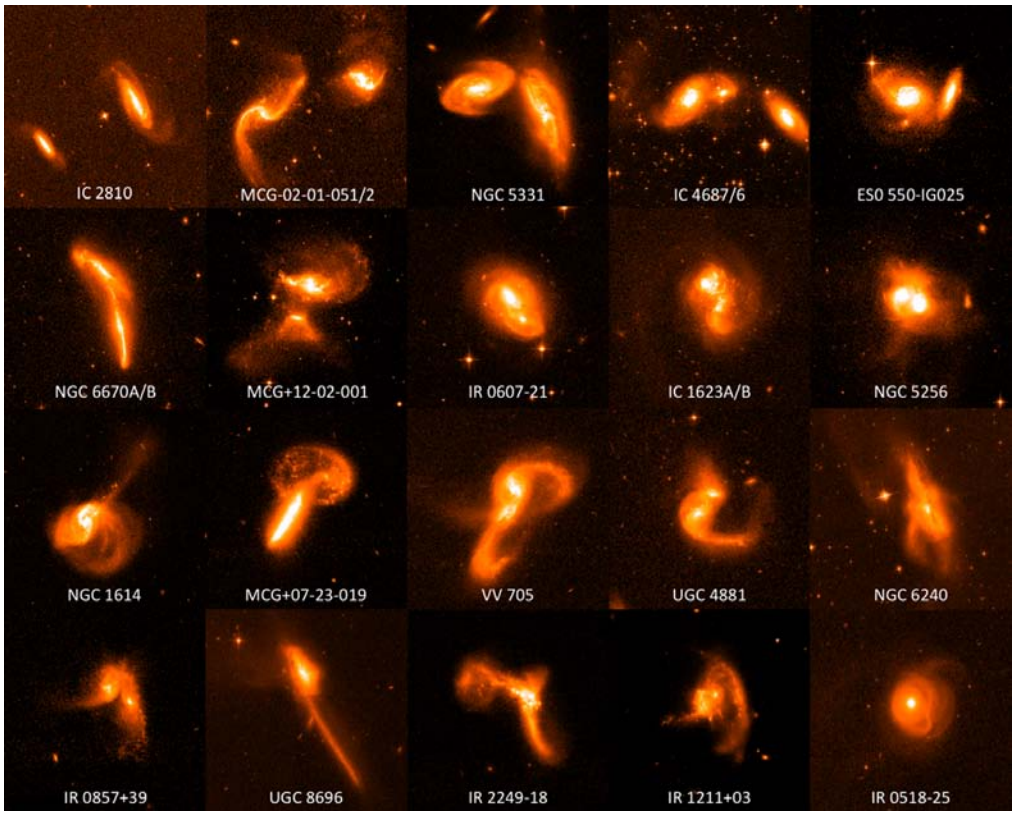

Figure 4. *HST*-ACS *I*-band images from the *HST*-GOALS" survey (Evans et al. 2009), in order of increasing log $(L_{\rm IR}/L_{\odot}) = 11.0 - 12.4$ (left-to-right, top-to-bottom). These data, which are part of the overall GOALS Legacy Survey (Armus et al. 2009), represent the subset of $\sim$ 90 "major mergers" that are a targeted part of our investigations with *Spitzer, HST, GALEX,* and *Chandra*. These images illustrate the progression from relatively widely spaced pairs, close to, or just after first pericenter passage that dominate the morphology of objects at the lower end of this luminosity range, through more advanced stages where double-nucleus objects are found embedded in largely overlapping disks, and finally to advanced mergers, which are characteristic all of the objects at the highest infrared luminosities.

out the merger disks along with the growing importance of AGN activity during the late stages of the merger process.

3.2. Nuclear Gas Concentrations

Millimeter-wave single-dish (CO) observations of complete samples of nearby LIRGs (e.g. Sanders et al. 1991, Solomon et al. 1997, Gao & Solomon 2004) have shown that all of these objects are molecular gas rich, with implied molecular gas masses $\log[M(H_2)/M_\odot)] \sim 9.5-10.5$. Initial millimeter-wave interferometer observations showed the then somewhat surprising result that for virtually all of the most luminous objects, the bulk of this gas was concentrated within the inner few kpc of the merger nucleus (see Scoville, this volume for a more complete discussion). Fig. 5 illustrates two contrasting examples of the CO distributions seen in major mergers: (1) NGC 4038/9 ("The Antennae"), a LIRG where large off-nuclear gas concentrations are detected, particularly in the disk overlap region of this intermediate-stage merger pair, while only relatively modest molecular gas concentrations are associated with the individual nuclei, and (2) the ULIRG/IR-QSO Mrk 231, where nearly all of the molecular gas is concentrated in the central kpc of the single nucleus of this advanced merger system. The creation of massive off-nuclear and extreme nuclear gas concentrations during major gas-rich mergers is now understood (e.g. Barnes & Hernquist 1992) as a natural consequence of collisional dissipation of angular momentum, where as much as 40-90% (depending largely on the initial rotation geometry of the merger) of the gas in the inner disks of the merging spirals ends up in the inner few kpc of the merger remnant.

High resolution mapping of the dense nuclear gas concentrations in (U)LIRGs are obviously required if one is to gain a better understanding of the relative contribution of starburst and AGN to the intense thermal dust emission at FIR-submm wavelengths, which dominates the bolometric luminosity of these objects. Resolutions of $10-100$ milliarcsec, corresponding to spatial scales of $\sim 10-100$ pc for ULIRGs in the RBGS, will be required in order to properly constrain the density and kinematics of the gas and the distribution of luminosity, and to provide theorists with a realistic picture of the extreme conditions in these dense cores. We are only now beginning to approach these scales with existing mm-submm interferometers, and then only for the brightest and nearest sources. But if the latest high resolution submm map of the nearest ULIRG, Arp 220, is any indication of what is to come, then it is clear that we may be in for new surprises. The new SMA 850μm map of Arp 220 at $\sim$200milliarcsec resolution (Sakamoto et al. 2008: see Scoville, this volume) clearly shows that the distribution of luminosity is much more compact than the distribution of gas and dust, with as much as $L_{IR} = 10^{12} L_\odot$ confined to a region of $\sim$30 pc diameter centered on the western nucleus. Pure starburst models clearly must be pushed to explain these new observations (see the contribution by Thompson, this volume), while models of AGN accretion disks will need to be tuned to match the new data (see the contribution by Duschl & Strittmatter, this volume). In the end, we may still find that both starbursts and AGN contribute substantial amounts of heating in these very extreme regions, but it seems clear that there are still exciting times ahead for framing the "starburst vs. AGN" debate.

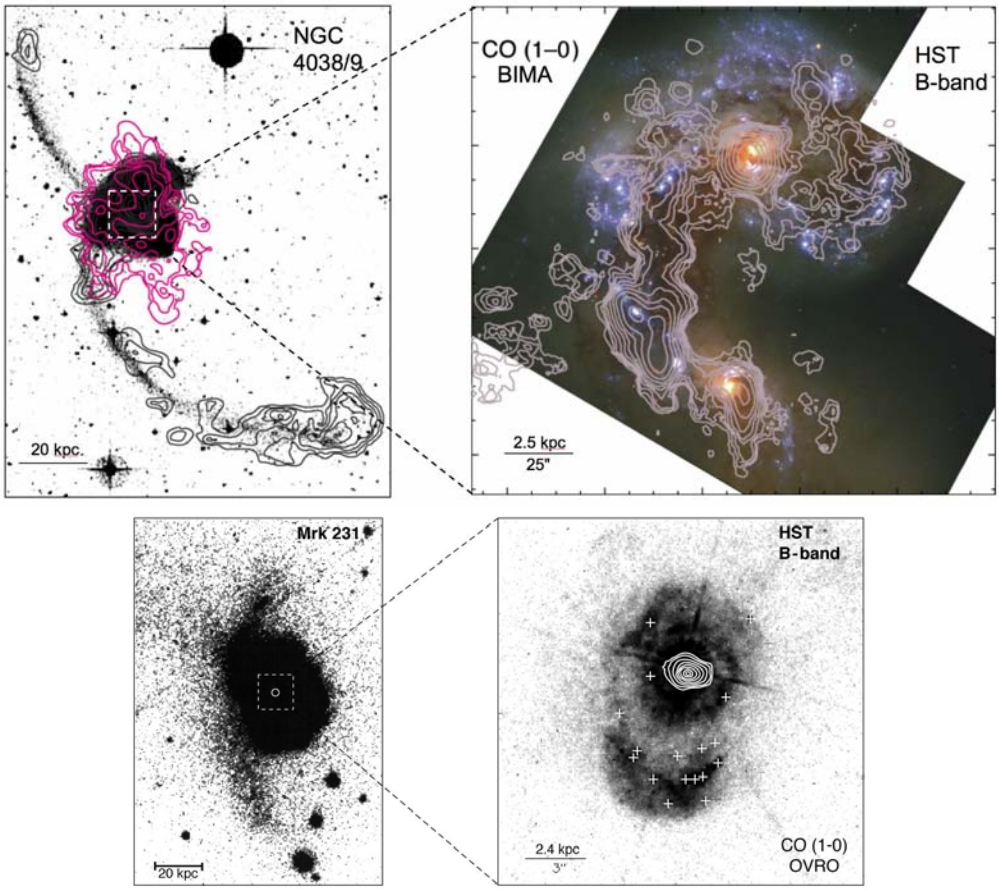

Figure 5. *(Top panels):* The intermediate stage merger NGC 4038/39 ("The Antennae"). The top left panel shows the deep optical image from Schweitzer (1978) with superimposed contours of HI 21-cm line emission (Hibbard & van Gorkom 1996) and soft X-Ray emission (Read et al. 1995), while the right panel shows the *HST* B-band image with contours of CO(1-0) emission (Gruendl et al. 1998) superimposed. *(Bottom panels):* The advanced merger/ULIRG/QSO Mrk 231. The left bottom panel shows the optical image from Sanders et al. (1987), along with the CO contour from Scoville et al. (1989). The right panel shows the *HST* B-band image and identified stellar clusters (+) from Surace et al. (1998), and high resolution CO contours from Bryant & Scoville (1996).

3.3. Starburst-AGN "Composites"

While it is clear that higher spatial resolution data can greatly improve our understanding of (U)LIRGs, there is still room for substantial improvement in our ability to interpret existing lower resolution multi-wavelength data. One prominent example comes from the recent construction of new, more realistic starburst models for interpreting standard optical emission line diagnostic ratios (e.g. [OIII]/Hβ vs. [NII]/Hα), coupled with the recent availability of extremely large and homogeneous spectrophotometric data sets such as that provided by the *Sloan Digital Sky Survey* (SDSS: York et al. 2000).

A new diagnostic scheme proposed by Kewley et al. (2006: KE06) recognizes a new class of starburst-AGN "Composite" galaxies, which substantially changes the boundary between low-ionization emission line galaxies (LINERS) and narrow-line Seyferts. Previous classification schemes resulted in a large fraction (30-40%) of infrared-selected galaxies at all infrared luminosities being classified as LINERS, while the new classification methods show that nearly all of these objects are more correctly described as starburst-AGN "Composities", where the relative strength of the AGN increases with increasing infrared luminosity. Fig. 6 from Yuan et al. (2009) illustrates the difference between the old and new narrow-line classification schemes, showing the location of ULIRGs with respect to the general population of SDSS emission-line galaxies, and the resulting percentage classifications of all infrared-selected galaxies (including broad-line Seyfert1s) versus infrared luminosity.

4. Concluding Remarks

A consistent picture of the cosmic importance of (U)LIRGs is now emerging from followup studies of large numbers of FIR-submm sources that have been detected in satellite and ground-base surveys, but it remains to be seen whether models being developed for low-z sources will still apply for the faint sources now being discovered at high-redshift. In this overview of LIRGs we have emphasized the following:

1) The population of ULIRGs evolves strongly with redshift such that their co-moving space density is $\sim$500$\times$ larger at $z \sim 2$ than that observed in the local universe.

2) Multi-wavelength, high-resolution studies of local (U)LIRGs confirm that strong interactions and mergers of gas-rich spirals are the trigger for these objects, and that the most luminous sources may be powered primarily by extremely compact nuclear sources. New, more realistic models of extreme starbursts as well as more realistic models of AGN accretion in massive self-gravitating disks will be required to explain these sources.

3) Deep *Spitzer*-MIPS surveys have identified thousands of (U)LIRGs over the redshift range $z \sim 0 - 3$. The properties of these sources are still being investigated, but their FUV-FIR SEDs show a broad range of spectral continuum shapes which appear to bridge the gap between "cool Arp 200-like" and "warm Mrk 231-like" SEDs.

4) New chemical evolution models applied to traditional optical line diagnostic diagrams for starburst and narrow-line AGN have identified a new class of starburst-AGN "Composite" galaxies. A reanalysis of the emission line spectra

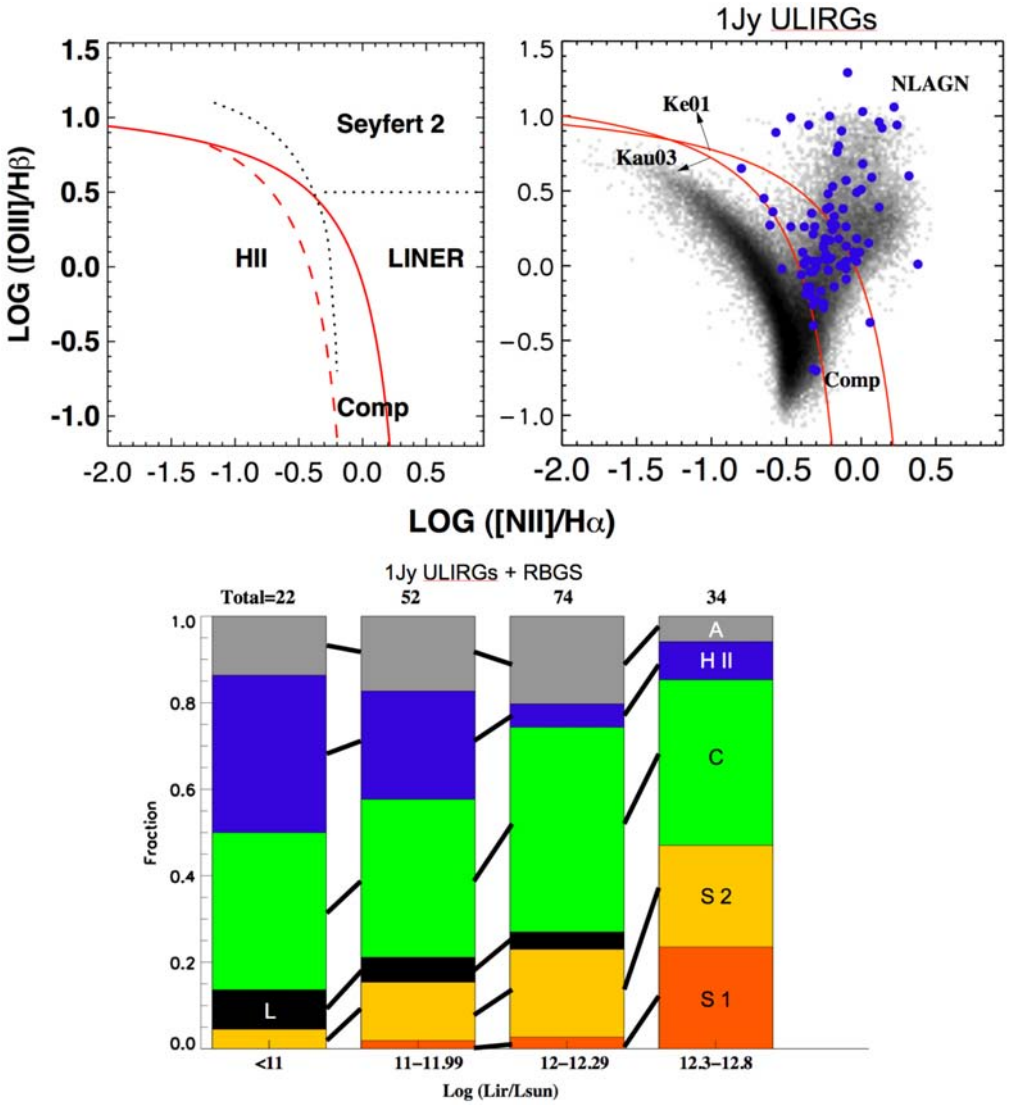

Figure 6. [Adapted from Yuan et al. (2009).] *Top panels:* Standard optical line diagnostic diagram. The top left panel shows the previous optical classification boundaries suggested by Veilleux & Osterbrock (1987) (black dotted lines separating Seyfert 2, LINER, HII), along with the new modified scheme proposed by Ke06. The Ke06 scheme includes a theoretical maximum starburst line (solid curve) and semi-empirical upper boundary for star-forming galaxies (dashed curve), from Kewley et al (2001) and Kauffmann et al. (2003), respectively. The Ke06 scheme substantially changes the LINER boundaries, and includes a class for starburst-AGN composites (labeled Comp). Note also that the Veilleux & Osterbrock (1987) scheme distinguishes between Seyfert 2 galaxies and LINERs, while the Ke06 classification scheme does not. The top right panel shows SDSS galaxies (small black dots) and the sample of 1-Jy ULIRGs (large black dots) using the Ke06 classification scheme. *Bottom panel:* Spectral type as a function of $L_{\rm IR}$ for infrared galaxies in the RBGS and 1 Jy samples using the new Ke06 classification scheme (S1=Seyfert 1, S2=Seyfert 2, C=Composite, L=LINER, HII=starburst, A=ambiguous).

of (U)LIRGs shows that the large percentage (∼30-40%) of previously identified LINERS are nearly all reclassified as starburst-AGN Composite galaxies, where the relative strength of the AGN increases with increasing infrared luminosity.

During the coming decade we can look forward to using new observing facilities such as the *Herschel Space Telescope*, the 50m *Large Millimeter Telescope* and the *Atacama Large Millimeter Array*, which offer great promise for greatly improving our understanding the importance of both starburst and AGN for the origin and evolution of (U)LIRGs.

Acknowledgments. Support for this work was provided in part by NASA through contracts 1282612 1298213 and 1344920 issued by the Jet Propulsion Laboratory. It is a pleasure to acknowledge the hospitality of Shanghai Normal University in sponsoring and organizing this international conference. We would also like to recognize the contributions from all of the members of the GOALS and S-COSMOS Teams for their help in these projects.

References

Armus, L. et al. 2009, PASP, in press, (arXiv0904.4498A)
Barnes, J.E. & Hernquist, L.E. 1992, ARA&A, 30, 705
Bryant, P.M. & Scoville, N.Z. 1996, ApJ, 457, 678
Evans, A.S. et al. 2009, AJ, submitted
Frayer, D.T. et al. 2009, AJ, in press, (arXiv0902.3273F)
Gao, Y. & Solomon, P.M. 2004, ApJS, 152, 63
Gruendl, R.A. et al. 1998, BAAS, 192, 6905
Hibbard, J. & van Gorkom, J. 1996, AJ, 111, 655
Jacobs, B.A. et al. 2009, AJ, submitted
Kartaltepe, J.S. 2009, PhD. Thesis, University of Hawaii
Kauffmann, G. et al. 2003, MNRAS, 346, 1055
Kewley, L.J., Groves, N., Kauffmann, G. & Heckman, T. 2006, MNRAS, 372, 961 (Ke06)
Kewley, L.J. et al. 2001, ApJ, 556, 121
Kim, D-C. & Sanders, D.B. 1998, ApJS, 119, 41
Neugebauer, G. et al. 1984, ApJ, 278, L1
Reed, A.M., Ponman, T.J. & Wolstencroft, R.D. 1995, MNRAS, 277, 397
Sakamoto, K. et al. 2008, ApJ, 684, 957
Sanders, D.B. 2003, JKAS, 36, 149
Sanders, D.B. & Mirabel, I.F. 1996, ARA&A, 34, 749 (SM96)
Sanders, D.B., Scoville, N.Z. & Soifer, B.T. 1991, ApJ, 370, 158
Sanders, D.B. et al. 1987, ApJ, 312, L5
Sanders, D.B. et al. 1988a, ApJ, 325, 74
Sanders, D.B., et al. 1988b, ApJ, 328, L35
Sanders, D.B., et al. 2003, AJ, 126, 1607 (RBGS)
Sanders, D.B. et al. 2007, ApJS, 172, 86
Schechter, P. 1976, ApJ, 203, 297
Schweizer, F 1978, IAUS, 77, 279
Scoville, N.Z. et al. 1989, ApJ, 345, L25
Scoville, N.Z. et al. 2007, ApJS, 172, 1
Solomon, P.M., Downes, D, Radford, S.J.E. & Barrett, J.W. 1997, ApJ, 478, 144
Surace, J.A. et al. 1998, ApJ, 492, 116
U, V. et al. 2009, AJ, submitted
Veilleux, S. & Osterbrock, D.E. 1987, ApJS, 63, 295
York, D.G. et al. 2000, AJ, 120, 1579
Yuan, T., Kewley, L.J. & Sanders, D.B. 2009, ApJ, submitted

David Sanders

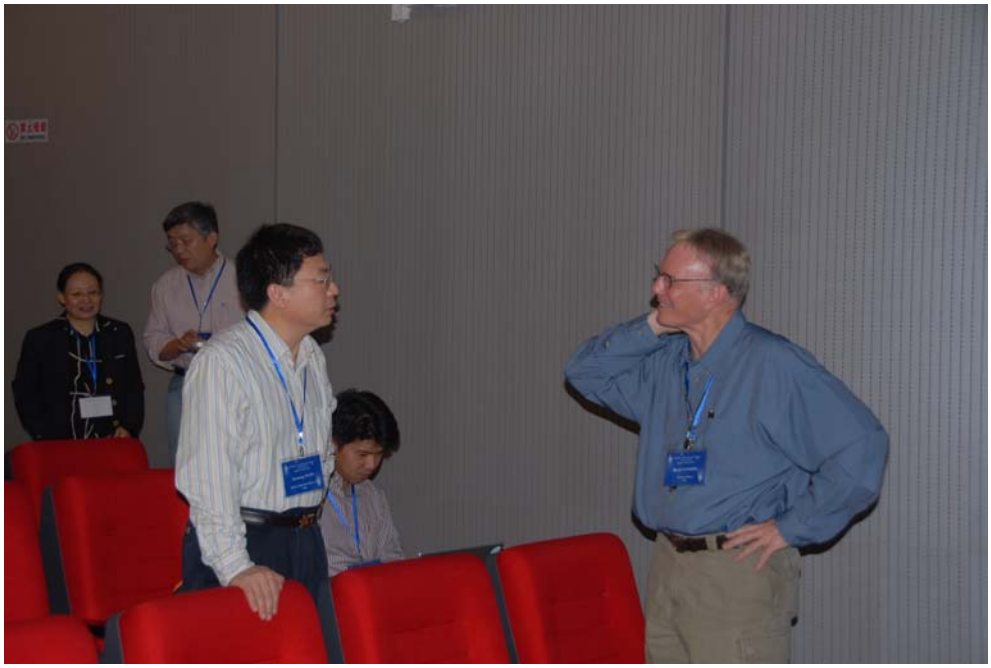

Jianmin Wang and David Sanders